HEI
COMMUNICATIONS

# New Methods in Ozone Toxicology: Abstracts of Six Pilot Studies



Health Effects Institute

Number 1 April 1992

## Background for the Ozone Toxicology Pilot Studies

Ozone, a significant component of urban smog, is produced when nitrogen oxides and hydrocarbons from motor vehicle emissions and other sources react with oxygen and sunlight. These reactions can produce peaks of ozone that exceed the National Ambient Air Quality Standard (NAAQS) for ozone, which is an average of 0.12 parts per million (ppm) for one hour, not to be exceeded more than once per year (U.S. Environmental Protection Agency 1991). Based on figures for 1990, approximately 25 percent of the U.S. population resides in areas that currently exceed the NAAQS for ozone.

Because substantial uncertainty exists regarding the potential health risks of long-term ozone exposure for large segments of the U.S. population, the Health Effects Institute (HEI) and the California Department of Health and Human Services nominated ozone for carcinogenicity testing by the National Toxicology Program (NTP). Both institutions were interested in ozone's potential to act as a carcinogen or cocarcinogen because its reactive properties suggest that this oxidant may act as a cancer initiator or promoter. The NTP subsequently approved a standard inhalation bioassay to evaluate the carcinogenic potential of ozone. Rats and mice would be exposed for 24 or 30 months to 0.0, 0.12, 0.5, or 1.0 ppm ozone, concentrations representing the current NAAQS for ozone as well as levels approximately four and eight times this level. The NTP also approved a cocarcinogenicity study using ozone and a known respiratory tract carcinogen found in tobacco smoke to evaluate whether ozone increases the risk of cancer development.

Both HEI and the NTP recognized that this bioassay presented a unique opportunity for a collaborative arrangement to study the effects of chronic ozone exposure. A major advantage of this collaboration for HEI would be to obtain animals that had been exposed to ozone under the rigorously controlled conditions required by the NTP. The NTP similarly would benefit by expanding the breadth of scientific information that could be gathered from these animals beyond the cancer endpoints usually evaluated by NTP.

As an initial phase of this mutual effort, HEI supported a group of pilot studies that were solicited through its RFA 89–2, "Health Effects of Chronic Ozone Inhalation: Collaborative NTP-HEI Studies. Phase I. Pilot Studies and Preproposals." The pilot studies allowed investigators to test the feasibility of their proposed methods for the valuable, although aged and potentially fragile, animals that would be available later from the chronic exposure study. To minimize the time needed for developing methods, HEI requested that investigators propose procedures that were already in use in their laboratories. The proposed methods were to be sufficiently sensitive to detect subtle alterations caused by ozone in the lungs or other tissues. HEI also was interested in proposals that incorporated new and innovative research approaches to evaluate ozone toxicity, such as those developed for molecular biology.

Lippmann (1989) and Tilton (1989) have reviewed the known effects of ozone exposure on humans and animals in recent articles. In clinical studies with exercising human subjects, acute ozone exposure produces a spectrum of reversible symptoms, including cough, shortness of breath, and pain on deep inspiration, even at ozone concentrations near the NAAQS. Alterations in lung function and an influx of inflammatory cells into the lungs have also been observed. However, current scientific evidence has not yet determined the effects of repeated exposures for many years to ozone concentrations that approximate or exceed the NAAQS.

Longer exposures of laboratory animals provide evidence that ozone produces cell injury and connective tissue alterations in the lungs (reviewed by Lippman 1989, and Tilton 1989). However, the mechanisms of these responses and whether such responses have long-term implications for the development of chronic lung diseases in humans, such as pulmonary fibrosis, are not known. Previous investigators, often using ozone exposure concentrations that exceeded the current NAAQS, have reported that the extent of injury depends on the ozone concentration. As the ozone exposure concentration decreases and approaches the NAAQS, the effects become more subtle and more difficult to detect. The question remains whether the extrapolation of the effects reported from animal studies is relevant to the long-term effects of ozone exposure at levels near the current NAAQS in humans.

As a group, the HEI pilot studies focused on methods to understand the mechanisms that account for the structural and biochemical

alterations in lung tissues caused by chronic ozone exposure. These studies included two morphometry projects to develop new procedures for quantifying structural changes in the lungs (Pinkerton and Vincent). A biochemical study evaluated the sensitivity of new assays for detecting DNA and RNA adducts, potential biomarkers for genetic damage induced by ozone exposure (Floyd). Another study evaluated methods for testing lung function in aged rats (one year old) after a brief ozone exposure (Uchida). Two immunocytochemistry studies were also approved. One study evaluated alterations in the site-specific expression of genetic message for lung structural proteins after ozone exposure (Parks). The second study tested new immunocytochemical labeling procedures for detecting the distribution of structural proteins in the lung interstitial matrix using electron microscopy (Chang).

Batelle Pacific Northwest Laboratories, the exposure facility for the NTP study, generously provided several of the pilot study investigators with samples of rat lung tissue obtained after a two-month exposure to ozone. In addition, all of the pilot study investigators were encouraged to request animals from the chronic exposure study by responding to RFA 90–1, "Health Effects of Chronic Ozone Inhalation: Collaborative NTP-HEI Studies, Phase II. Full Proposals." Methods tested under the pilot studies then could be used in the full-scale investigation. Three of the pilot study investigators (Chang, Parks, and Pinkerton) were subsequently funded under RFA 90–1.

The unifying focus of this group of six pilot studies is the exploration of new methods for evaluating the potentially subtle effects of ozone exposure in the lungs. All of the investigators funded under RFA 89–2 submitted final reports that were reviewed by the HEI Health Review Committee. The Committee decided that, because the pilot studies were brief and exploratory in nature, external peer review of the reports was unnecessary. The purpose of this HEI Communication is to provide brief summaries of the findings presented in those reports. The format provides an extended abstract of each final report prepared by the respective investigators, followed by comments on the study by the Health Review Committee. Copies of the final reports are available from HEI on request.

The findings of the pilot studies provide information about the feasibility of new techniques for evaluating the toxicity of ozone. Such information may ultimately be used to assess the potential risks to human health associated with ozone exposure and to formulate a relevant NAAQS for this oxidant.

## References

Lippmann M. 1989. Health effects of ozone: A critical review. J Air Pollut Control Assoc 39:672–695.

Tilton BE. 1989. Health effects of tropospheric ozone. Environ Sci Technol 23:257–263.

U.S. Environmental Protection Agency. 1991. National Air Quality and Emissions Trends Report, 1990. Office of Air Quality Planning and Standards, Research Triangle Park, NC.

U.S. Office of Technology Assessment. 1988. Urban Ozone and the Clean Air Act: Problems and Proposals for Change. Oceans and Environment Program, Office of Technology Assessment, United States Congress, Washington, DC.

# Immunocytochemical Study of the Connective Tissue of Rat Lungs

*Ling-Yi L. Chang and James D. Crapo*
*Department of Medicine*
*Duke University, Durham, NC 27710*

## Introduction

Subchronic and chronic exposures to ozone have been shown to cause interstitial remodeling (Gross and White 1987; Chang et al. 1989). Some important questions concerning the interstitial changes induced by chronic exposure to ozone ($O_3$) are whether such exposures cause chronic pulmonary injury and whether these injuries are fibrotic or emphysematous in nature. One approach to these questions is to define and quantify the changes in the interstitial matrix after exposure to $O_3$ by using protein A–gold immunocytological techniques to label collagens and elastin. We undertook to develop protocols for the immunocytochemical localization of elastin and collagen types I, III, and IV in rat lungs. Our goals were:

1. to establish a proper fixation protocol for conducting both morphometric analysis and immunocytochemical studies of the matrix proteins on the same lung tissue;
2. to determine the most suitable embedding medium for optimal immunocytochemical detection and quantification of matrix proteins in the lung;
3. to demonstrate labeling of matrix proteins on sections of rat lungs; and
4. to devise sampling strategies for measuring relative labeling densities of the matrix proteins.

## Methods

**Histology** Rat lungs were fixed by intratracheal instillation of fixatives (Hyatdavoudi et al. 1980). Lung tissue was processed for morphometric and immunocytochemical studies. Tissue blocks for electron microscopic morphometry were post-fixed with osmium tetraoxide ($OsO_4$) and embedded in Epoxy resin. Morphometric analyses were carried out by the methods described by Pinkerton and Crapo (1985). Blocks for immunocytochemistry were processed by a variety of methods to test the effects of cross-linking reagents, fixative time, embedding materials, and embedding temperature on antigenicity. Labeling was also done on 8-μm-thick cryostat sections.

**Immunocytochemistry** Rabbit antibodies to rat type I collagen, rat type III collagen, and mouse type IV collagen were purchased from Biodesign International (Kennebunkport, ME); both whole sera and the IgG fraction were obtained. Rabbit antisera to rat lung elastin was purchased from Elastin Products (Owensville, MI). In addition, a rabbit antisera to monkey type I collagen and an affinity-purified antibody to human type I collagen were obtained from Dr. Detlef Schuppan (Free Berlin University, Berlin, Germany). Ultrathin sections were incubated successively with one of the specific antibodies for a matrix protein and with protein A–gold (9 nm). After each incubation, the sections were rinsed with phosphate-buffered saline (Slot et al. 1989).

## Results

After measuring the osmolarity of various concentrations of formaldehyde, glutaraldehyde, and several types of buffer, we selected 1 percent paraformaldehyde and 0.2 percent glutaraldehyde in 0.1 M phosphate buffer (pH 7.4) as the primary fixative. This fixative has an osmolarity of 510 mOsm and did not appear to block immunolabeling of matrix proteins on thick frozen sections. Morphometric analysis was conducted on rat lung tissue treated with this fixative. The data were compared with those obtained from tissue fixed with 2 percent glutaraldehyde in 0.085 M cacodylate buffer (350 mOsm). We found that, although the total volumes of various lung parenchymal tissues measured by volume displacement methods (Pinkerton and Crapo 1985) were not altered significantly, the ratios of epithelium, interstitium, endothelium, and capillary lumen volumes were changed. In addition, the surface density and total surface area of alveolar basement membrane were doubled. These results suggest that uneven shrinkage of tissue and compression of alveolar septa occurred during processing.

For the immunocytochemical studies, tissue was fixed with the 1 percent paraformaldehyde and 0.2 percent glutaraldehyde mixture for one hour and then transferred to 2 percent paraformaldehyde. Fixation by glutaraldehyde was needed to preserve the structural integrity of the alveolar septum. However, extensive treatment with glutaraldehyde destroys protein antigenicity.

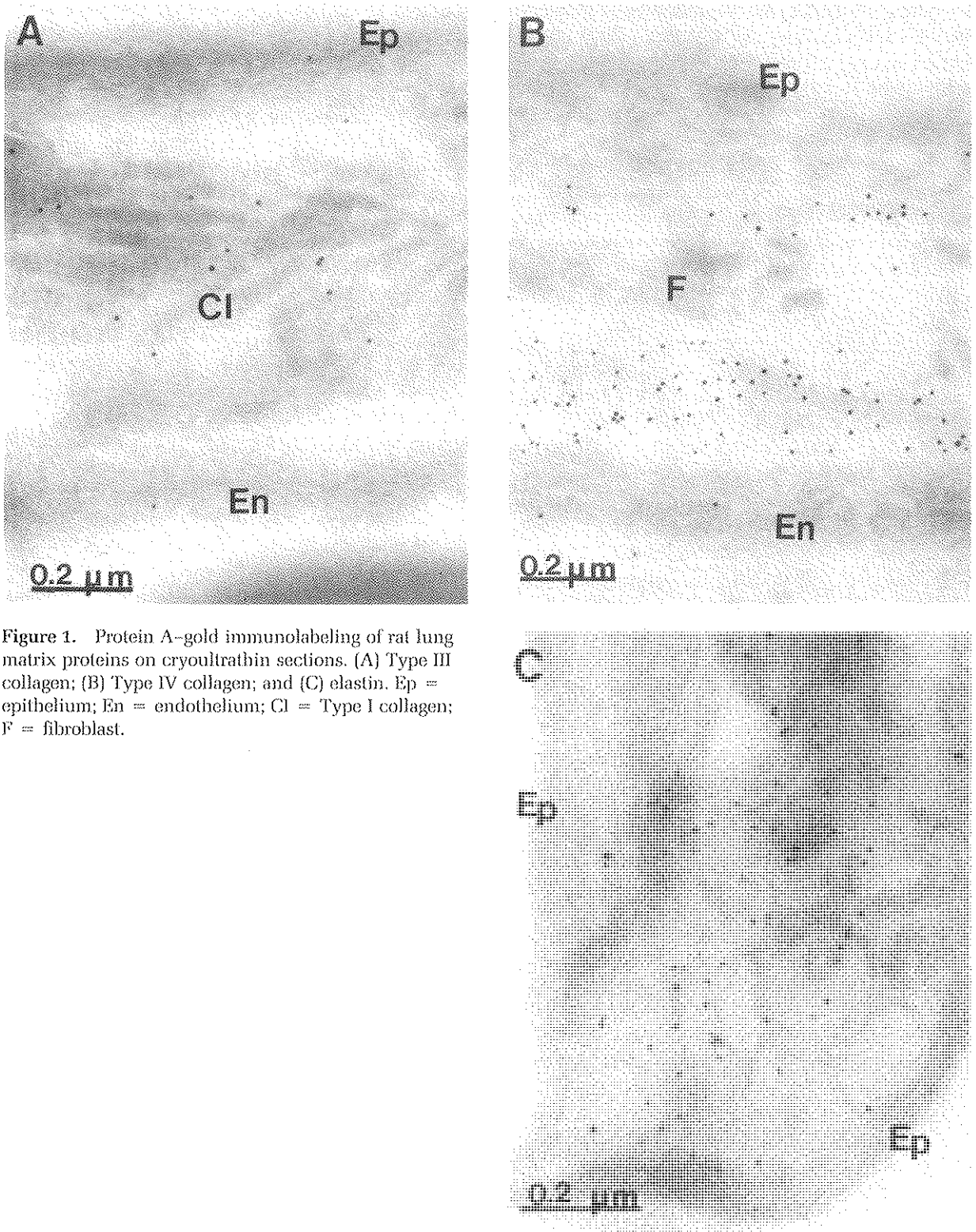


**Figure 1.** Protein A–gold immunolabeling of rat lung matrix proteins on cryoultrathin sections. (A) Type III collagen; (B) Type IV collagen; and (C) elastin. Ep = epithelium; En = endothelium; Cl = Type I collagen; F = fibroblast.

Therefore, we used a low concentration of glutaraldehyde for a brief time and transferred the tissue to paraformaldehyde containing fixative. Tissues fixed with 2 percent paraformaldehyde in 0.1 M phosphate buffer were used as controls for the labeling studies. The following results were found:

1. Immunocytochemical localization of type I collagen was not demonstrated on ultrathin sections of rat lung tissue, regardless of the type or duration of fixative used, or the embedding material or embedding temperature. Labeling of type I collagen was detected by light microscopy on 8-μm cryostat sections.
2. The duration of fixation greatly influenced the antigenicities of type III collagen, type IV collagen, and elastin. Fixation for longer than four hours abolished labeling for type IV collagen and reduced the labeling densities for type III collagen and elastin.
3. Embedding in LR White resin destroyed the immunoreactivity of type III and type IV collagens, but did not affect elastin.
4. Labeling of type III collagen codistributed with type I collagen in the alveolar interstitium. Type IV collagen was localized exclusively in the basement membranes of the epithelium and endothelium. Immunolabeling of elastin was found primarily on septal tips but was also observed with alveolar septa (Figure 1).

## Discussion

We carried out experiments to establish fixation and embedding procedures for the immunocytolabeling of lung interstitial matrix proteins. We found that type III collagen, type IV collagen, and elastin were sensitive to long durations of fixation, but tolerated only a low concentration of glutaraldehyde. On the other hand, all available antibodies to type I collagen failed to yield specific labeling of the antigen that could be recognized at the electron microscopic level. Both the antisera and the IgG fraction for anti–type I collagen gave positive labeling on 8-μm cryostat sections. The labeling observed at the light microscopic level may have been nonspecific, although Western blot analysis of the antibodies using sodium-dodecyl-sulfate polyacrylamide gel electrophoresis showed monospecificity of labeling. Another explanation for this apparent contradiction between electron and light microscopic immunolabeling is that type I collagen antigenicity may be extremely sensitive to the duration of fixation (Clement et al. 1985), resulting in few active epitopes available in the ultrathin sections used for immunodetection. We will continue to test the effects of shorter fixation durations on the efficacy of immunolabeling of type I collagen.

Our results suggest that anisotropic shrinkage of lung tissue occurred when lung tissue was fixed by 1 percent paraformaldehyde and 0.2 percent glutaraldehyde (510 mOsm). A further reduction of osmolarity could be achieved by decreasing the concentration of formaldehyde to 0.5 percent. However, this is not desirable because tissue structure preservation is not optimal for electron microscopic immunocytochemistry and morphometry when such a low concentration of fixative is used. Absolute quantification of matrix proteins is very difficult to measure because the same tissue section cannot be used for both morphometry and immunocytochemistry. However, relative quantification of matrix proteins still can be performed; we have devised quantification procedures for the matrix proteins collagens III and IV, and elastin. We recommend that some animal tissue from the NTP-Health Effects Institute chronic ozone exposure study be fixed by the stepwise fixation protocol, which is optimally effective for immunocytochemical investigations of the matrix proteins.

## References

Chang L, Huang Y, Stockstill B, Crapo JD. 1989. Effects of chronic exposure to an ambient pattern of $O_3$ on rodent lungs (abstract). Toxicologist 9:44.

Clement B, Rissel M, Peyrol S, Mazurier Y, Grimaud J, Guillouzo A. 1985. A procedure for light and electron microscopic intracellular immunolocalization of collagen and fibronectin in rat liver. J Histochem Cytochem 33:407–414.

Gross KB, White JH. 1987. Functional and pathologic consequences of a 52-week exposure to 0.5 ppm ozone followed by a clean air recovery period. Lung 165: 183–295.

Hayatdavoudi G, Crapo JD, Miller FJ, O'Neil JJ. 1980. Factors determine degree of inflation in intratracheally fixed rat lungs. J Appl Physiol 48:389–393.

Pinkerton KE, Crapo JD. 1985. Morphometry of the alveolar region of the lung. In: Handbook of Experimental Pharmacology, Vol. 75, (Witschi HP, Brain JD, eds.) pp. 259–285. Springer-Verlag, New York, NY.

Slot JW, Posthuma G, Chang L, Crapo JD, Geuze HJ. 1989. Quantitative aspects of immunogold labeling in embedded and in nonembedded sections. Am J Anat 185:271–281.

## HEI COMMENTS

The objective of this study was to develop procedures for labeling elastin and type I, type III, and type IV collagens with antibody–gold particle complexes on ultrathin sections of lung tissue. These complexes then could be quantified by electron microscopy to determine the site-specific amounts and distribution patterns of these interstitial matrix components in lung tissue samples. Thraugh this study, these investigators wanted to extend their methods in lung morphometry and develop procedures for quantifying interstitial matrix proteins.

Using commercial antibodies, the investigators devised fixation procedures that yielded successful labeling of elastin and type III and type IV collagens, but not type I collagen. An explanation for the failure to label type I collagen with the antibody-gold complex was not provided. The observed labeling patterns for elastin and type III and type IV collagens corresponded with known distribution patterns for these lung proteins. However, these procedures must be tested to ascertain their utility for other investigators because different antibodies often require different fixation procedures.

The authors acknowledged that their procedures provide an appraach for relative, but not absolute, quantification af interstitial proteins. They reported that the fixation procedures produced nonuniform shrinkage of the lung tissue that would compromise the accuracy of any subsequent morphometric studies. Studies comparing these results with results from tissue samples obtained after exposure to ozone or other toxic agents are a logical next step. Future studies to label other matrix components, such as laminin and fibronectin, would also be of interest.

# Ozone-Mediated Damage to Lung Nucleic Acids

*Robert A. Floyd, Quentin Pye, Lindsay Maidt, and Peter Wong*
*Molecular Research Program*
*Oklahoma Medical Research Foundation*
*Oklahoma City, OK 73104*

### Introduction

High levels of ozone in air are produced predominantly by photochemical reactions involving oxygen and atmospheric organic pollutants. In many urban areas, the concentration of ozone can reach levels in excess of 0.12 parts per million (ppm) several times during the year. Ozone is very toxic to many plants and, when inhaled, damages lungs. The exact mechanisms involved in ozone-mediated lung injury are unknown; however, considerable evidence clearly implicates oxidative mechanisms. Recent observations of tissue damage indicate mechanisms that are triggered by ozone and mediated by oxygen free radicals (Warren et al. 1988) and increases in xenobiotic metabolism in the lungs (Esterline et al. 1989). In addition, ozone has been shown to cause neoplastic transformation of cultured cells (Borek et al. 1986, 1989).

Attacks on DNA by oxygen free radicals cause strand breaks and base modifications, including the formation of 8-hydroxy-2'-deoxyguanosine (8-OHdG) in DNA. Our laboratory has been very involved actively over the last five years in research directed toward understanding oxidative damage to nucleic acids. The research effort has concentrated on (1) developing a very sensitive method of quantifying 8-OHdG in DNA (Floyd et al. 1986a,b); (2) examining the formation of 8-OHdG in isolated DNA (Floyd et al. 1988, 1989a); (3) evaluating the significance of 8-OHdG within the DNA of living systems (Floyd et al. 1986a, 1989b); and, more recently, (4) characterizing the formation and significance of 8-hydroxyguanosine (8-OHG) in RNA. Nishimura and associates showed that the formation of 8-OHdG in DNA is closely associated with cancer development in a number of cases (Kasai et al. 1987). We have reviewed this area (Floyd 1990 a,b) and find significant support for the concept.

The presence of 8-hydroxyguanine within DNA or RNA, may have significant consequences in biological systems. It is, therefore, important to determine whether ozone-induced injury is

mediated in part by the formation of this modified base in nucleic acids of injured tissue. We have conducted extensive experiments that demonstrated increased 8-OHdG content of chloroplast DNA from ozone-injured plants (Floyd et al. 1989b). The pertinent results for these experiments are (1) plants exposed to an acute dose (0.2 to 0.4 ppm) of ozone increase twofold in 8-OHdG content of chloroplast DNA; (2) illuminated chloroplasts exposed to ozone have an increase in 8-OHdG of chloroplast DNA nearly seven times that of controls exposed to air; and (3) isolated DNA exposed to ozone did not have an increased content of 8-OHdG, even though ozone reacted with the DNA. We also recently exposed isolated RNA to ozone and found no increased level of 8-OHG; however, exposure of rat lung microsomes to ozone did appear to cause an increase in the 8-OHG content of the microsomal RNA. These data again suggest that the influence of ozone on biological tissue is complex and probably involves a secondary generation of free radicals. The present pilot study was initiated to help resolve these questions.

The specific aim of this pilot study was to determine the 8-OHG content of lung RNA and DNA from rats exposed to various levels of ozone for two months and compare these values with those obtained from appropriate control animals receiving background levels of ozone. The animals were obtained from the Batelle Pacific Northwest Laboratories, Richland, WA.

## Methods

We studied the effects of long-term (two-month) ozone exposure on rats. Oxidative damage to lung RNA and DNA was assessed by analyzing the 8-OHG and 8-OHdG content of the RNA and DNA, respectively. The rat lungs for this study were made available at the termination of a study conducted by the Batelle Pacific Northwest Laboratories. That study examined the effects of long-term ozone exposure on rats. Rats were exposed for 2 months at three different levels of ozone: 0, 0.5, and 1 ppm. The animals were killed, and the lungs were stored at −70°C until used in the present study.

**Table 1. 8-Hydroxy-2'-deoxyguanosine Content of Rat Lung DNA from Rats Exposed to Ozone for Two Months**

| Gender | Exposure | 8-Hydroxy-2'-deoxyguanosine (pmol/μL) | Deoxyguanosine (pmol/μL) | 8-Hydroxy-2'-deoxyguanosine per $10^5$ Deoxyguanosine | Average[a] |
|---|---|---|---|---|---|
| Male | Control | 0.028 | 103.09 | 26.86 | |
| Male | Control | 0.055 | 286.85 | 19.33 | 21.57 ± 1.94 |
| Male | Control | 0.056 | 253.50 | 21.95 | |
| Male | Control | 0.048 | 263.26 | 18.13 | |
| Male | 0.5 ppm Ozone | 0.024 | 121.69 | 19.31 | |
| Male | 0.5 ppm Ozone | 0.034 | 229.39 | 14.86 | 18.28 ± 1.15 |
| Male | 0.5 ppm Ozone | 0.045 | 225.24 | 19.76 | |
| Male | 0.5 ppm Ozone | 0.037 | 193.55 | 19.21 | |
| Male | 1 ppm Ozone | 0.066 | 217.65 | 30.23 | |
| Male | 1 ppm Ozone | 0.041 | 231.25 | 17.61 | 22.22 ± 2.93 |
| Male | 1 ppm Ozone | 0.029 | 159.04 | 18.14 | |
| Male | 1 ppm Ozone | 0.049 | 215.66 | 22.91 | |
| Female | Control | 0.017 | 68.18 | 24.82 | |
| Female | Control | 0.043 | 178.12 | 23.95 | 20.40 ± 3.05 |
| Female | Control | 0.032 | 294.63 | 11.53 | |
| Female | Control | 0.046 | 218.28 | 21.30 | |
| Female | 0.5 ppm Ozone | 0.063 | 291.57 | 21.36 | |
| Female | 0.5 ppm Ozone | 0.055 | 272.60 | 20.20 | 20.55 ± 0.82 |
| Female | 0.5 ppm Ozone | 0.073 | 330.36 | 22.20 | |
| Female | 0.5 ppm Ozone | 0.068 | 369.89 | 18.43 | |
| Female | 1 ppm Ozone | 0.026 | 172.29 | 15.08 | |
| Female | 1 ppm Ozone | 0.037 | 232.42 | 16.18 | 18.58 ± 1.96 |
| Female | 1 ppm Ozone | 0.080 | 335.04 | 23.86 | |
| Female | 1 ppm Ozone | 0.060 | 313.71 | 19.20 | |

[a]Mean ± SD for each exposure group.

Lung tissue from rats exposed to various levels of ozone was shipped frozen and on dry ice from the Batelle Pacific Northwest Laboratories. The tissue was then stored at −80°C until analyzed. The tissue DNA and RNA were analyzed for 8-OHdG and 8-OHG, respectively, by first extracting DNA and RNA from a representative piece of each sample. The DNA and RNA were isolated from tissue using a cesium chloride ($CsCl_2$) gradient method. Briefly, the tissue (< 0.5 g) was homogenized in 3 mL of 1 mM sodium ethylenediaminetetraacetic acid (EDTA) and 1% sodium dodecylsulfate, pH 7.4, and then was allowed to stand at room temperature for at least one hour. This solution was then mixed with 4.16 g $CsCl_2$ and 620 μL 60% sucrose and brought to a final volume of 5 mL with 1 mM EDTA. This solution was placed over a 1-mL 5.7 M $CsCl_2$ cushion in 50Ti tubes and centrifuged in a Beckman (Fullerton, CA) L5-75 ultracentrifuge at 18°C for 20 hours at 36,000 rpm. DNA was isolated from the $CsCl_2$ supernatant by five times dilution and then salt and ethanol precipitation. The pellet contained the RNA that was recovered after salt and ethanol precipitation. DNA was digested to the nucleoside level using the method described by Beland and coworkers (1979), and RNA was digested to the nucleoside level by using the enzymes nuclease $P_1$ and acid phosphatase overnight at 37°C. The 8-OHdG and deoxyguanosine contents of DNA and the 8-OHG and guanosine contents of RNA were determined using high-pressure liquid chromatography with an ultraviolet detector positioned before an electrochemical detector. Two additional studies were done to determine whether in vitro ozone exposure caused formation of 8-OHG in RNA. Rat lung homogenates and rat liver homogenates were exposed to 0.5 ppm ozone by bubbling the gas into the tissue preparations. The RNA was then isolated using a cesium chloride ($CsCl_2$) gradient and analyzed for 8-OHG content.

**Table 2. 8-Hydroxyguanosine Content of Rat Lung RNA from Rats Exposed to Ozone for Two Months**

| Gender | Exposure | 8-Hydroxy-guanosine (pmol/μL) | Guanosine (pmol/μL) | 8-Hydroxy-guanosine per $10^5$ Guanosine | Average[a] |
|---|---|---|---|---|---|
| Male | Control | 0.027 | 444.8 | 6.10 | |
| Male | Control | 0.021 | 485.7 | 4.24 | 4.59 ± 1.36 |
| Male | Control | 0.016 | 466.6 | 3.43 | |
| Male | Control | ND[b] | ND | ND | |
| Male | 0.5 ppm Ozone | 0.021 | 428.6 | 4.90 | |
| Male | 0.5 ppm Ozone | 0.020 | 420.5 | 4.68 | 5.19 ± 0.97 |
| Male | 0.5 ppm Ozone | 0.025 | 547.6 | 4.56 | |
| Male | 0.5 ppm Ozone | 0.035 | 527.1 | 6.64 | |
| Male | 1 ppm Ozone | 0.022 | 470.5 | 4.76 | |
| Male | 1 ppm Ozone | 0.019 | 485.7 | 3.97 | 4.13 ± 0.49 |
| Male | 1 ppm Ozone | 0.019 | 450.9 | 4.21 | |
| Male | 1 ppm Ozone | 0.015 | 422.9 | 3.59 | |
| Female | Control | 0.018 | 346.3 | 5.20 | |
| Female | Control | 0.027 | 464.7 | 5.81 | 4.57 ± 1.27 |
| Female | Control | 0.014 | 488.3 | 2.87 | |
| Female | Control | 0.018 | 418.0 | 4.42 | |
| Female | 0.5 ppm Ozone | 0.037 | 439.3 | 8.42 | |
| Female | 0.5 ppm Ozone | 0.022 | 430.3 | 5.11 | 5.36 ± 2.14 |
| Female | 0.5 ppm Ozone | 0.011 | 253.2 | 4.34 | |
| Female | 0.5 ppm Ozone | 0.011 | 309.0 | 3.56 | |
| Female | 1 ppm Ozone | 0.023 | 436.4 | 5.27 | |
| Female | 1 ppm Ozone | 0.019 | 434.5 | 4.37 | 5.08 ± 0.72 |
| Female | 1 ppm Ozone | 0.031 | 516.7 | 6.00 | |
| Female | 1 ppm Ozone | 0.021 | 450.6 | 4.67 | |

[a]Mean ± SD for each exposure group.
[b]ND = Not done.

**Table 3. 8-Hydroxyguanosine Formation in RNA of Rat Lung Homogenate Exposed in Vitro to 0.5 ppm Ozone[a]**

| Exposure | Guanosine (pmol/μL) | 8-Hydroxy-guanosine (pmol/μL) | 8-Hydroxy-guanosine per $10^5$ Guanosine | Average |
|---|---|---|---|---|
| 0 | 420.8 | 0.047 | 11.2 | |
| 0 | 488.2 | 0.038 | 7.8 | 9.5 |
| 15 Minutes | 354.5 | 0.040 | 11.3 | |
| 15 Minutes | 416.9 | 0.046 | 11.0 | 11.2 |
| 60 Minutes | 443.0 | 0.068 | 15.3 | |
| 60 Minutes | 397.4 | 0.036 | 9.1 | 12.2 |

[a]Rat lung homogenate was exposed by bubbling 0.5 ppm ozone into the solution. The RNA was isolated using $CsCl_2$ gradient.

**Table 4. 8-Hydroxyguanosine Formation in RNA of Isolated Rat Liver Mitochondria Exposed in Vitro to 0.5 ppm Ozone[a]**

| Exposure | Guanosine (pmol/μL) | 8-Hydroxy-guanosine (pmol/μL) | 8-Hydroxy-guanosine per $10^5$ Guanosine | Average |
|---|---|---|---|---|
| 0 | 271.3 | 0.023 | 8.5 | |
| 0 | 308.0 | 0.023 | 7.5 | 8.0 |
| 15 Minutes | 469.5 | 0.043 | 9.2 | |
| 15 Minutes | 457.6 | 0.037 | 8.2 | 8.98 |
| 15 Minutes | 471.8 | 0.045 | 9.6 | |
| 30 Minutes | 422.5 | 0.060 | 14.2 | |
| 30 Minutes | 427.2 | 0.045 | 10.5 | 12.35 |
| 60 Minutes | 366.7 | 0.051 | 13.9 | |
| 60 Minutes | 352.6 | 0.040 | 11.3 | 12.48 |
| 60 Minutes | 353.3 | 0.038 | 10.8 | |

[a]Rat liver mitochondria were exposed by bubbling 0.5 ppm ozone into the solution. The RNA was isolated using $CsCl_2$ gradient.

## Results

The results of our first DNA and RNA analyses for a small number of the lung samples showed that the amounts of 8-OHdG in the lung DNA of male rats increased with increasing levels of ozone. This result, however, was not matched in the female animals. These early results suggested exciting possibilities.

We then conducted a more extensive analysis of 8-OHdG and 8-OHG levels in exposed animals. The results for the 8-OHdG content of DNA and the 8-OHG content of RNA from the lung tissues of rats exposed to various levels of ozone are shown in Tables 1 and 2, respectively. The data reveal that there is no correlation between either 8-OHdG or 8-OHG content of DNA or RNA and the exposures to ozone. Table 3 presents data for a rat lung homogenate that was exposed to 0.5 ppm ozone in vitro. RNA was then isolated from the homogenate using a $CsCl_2$ gradient. Compared with the data in Table 2, the 8-OHG content was higher and increased with longer ozone exposure times. Based on these data, we subsequently exposed isolated rat liver mitochondria to 0.5 ppm ozone in vitro and determined the 8-OHG content of RNA isolated by $CsCl_2$. The results, which are given in Table 4, similarly show an increase in 8-OHG levels with increasing duration of in vitro ozone exposure.

## Discussion

From the results of this pilot study, we conclude that a rigorous evaluation of the 8-OHdG and

8-OHG content of DNA and RNA from lungs of animals exposed to various levels of ozone is still needed. However, preliminary data suggest that these analyses may be valuable tools to assess the mechanism of ozone-mediated damage.

## References

Beland FA, Dooly KL, Casciano DA. 1979. Rapid isolation of carcinogen-bound DNA and RNA by hydroxyapatite chromatography. J Chromatogr 174:177–186.

Borek C, Ong A, Zaider M. 1989. Ozone activates transforming genes in vitro and acts as a synergistic co-carcinogen with gamma rays only if delivered after radiation. Carcinogenesis 10:1549–1551.

Borek C, Zaider M, Ong A, Mason H, Witz G. 1986. Ozone acts alone and synergistically with ionizing radiation to induce in vitro neoplastic transformation. Carcinogenesis 7:1611–1613.

Esterline RL, Bassett DJP, Trush MA. 1989. Characterization of the oxidant generation by inflammatory cells lavaged from rat lungs following acute exposure to ozone. Toxicol Appl Pharmacol 99:229–239.

Floyd RA. 1990a. Role of oxygen free radicals in carcinogenesis and brain ischemia. FASEB J 4:2587–2597.

Floyd RA. 1990b. The role of 8-hydroxyguanine in carcinogenesis. Carcinogenesis 11:1447–1450.

Floyd RA, Watson JJ, West M, Wong PK. 1986a. Formation of 8-hydroxydeoxyguanosine, hydroxyl free radical adduct of DNA in granulocytes exposed to the tumor promoter, tetradeconylphorbolacetate. Biochem Biophys Res Commun 137:841–846.

Floyd RA, Watson JJ, Wong PK, Altmiller DH, Rickard RC. 1986b. Hydroxyl free radical adduct of deoxyguanosine: Sensitive detection and mechanisms of formation. Free Radic Res Commun 1:163–172.

Floyd RA, West MS, Eneff KL, Hogsett WE, Tingey DT. 1988. Hydroxyl free radical mediated formation of 8-hydroxyguanine formation in isolated DNA. Arch Biochem Biophys 262:266–272.

Floyd RA, West MS, Eneff KL, Schneider JE. 1989a. Methylene blue plus light mediates 8-hydroxyguanine formation in DNA. Arch Biochem Biophys 273:106–111.

Floyd RA, West MS, Hogsett WE, Tingey DT. 1989b. Increased 8-hydroxyguanine content of chloroplast DNA from ozone-treated plants. Plant Physiol 91:644–647.

Kasai H, Nishimura S, Kurokawa Y, Hayashi Y. 1987. Oral administration of the renal carcinogen, potassium bromate, specifically produces 8-hydroxydeoxyguanosine in rat target organ DNA. Carcinogenesis 8:1959–1961.

Warren DL, Hyde DM, Last JA. 1988. Synergistic interaction of ozone and respirable aerosols on rat lungs: IV. Protection by quenchers of reactive oxygen species. Toxicology 53:113–133.

The purpose of this study was to determine whether ozone exposure damages the DNA or RNA of rat lung cells. The investigators assayed for a DNA adduct (8-hydroxy-2′-deoxyguanosine) and an RNA adduct (8-hydroxyguanosine) in lung tissue samples from rats previously exposed to ozone. An increase in the number of these adducts in the samples would indicate that ozone exposure caused oxidative damage to nucleic acids.

No consistent differences in either DNA or RNA adduct content were found in lung samples from male or female rats exposed to levels of up to 1 ppm ozone for 2 months when compared with matched controls. In contrast, RNA adduct content was up to 50 percent higher in samples of rat lung homogenates and liver mitochondria exposed to 0.5 ppm ozone in vitro compared with controls. Because the normal structural and biochemical environment of the lung cells is not present during an in vitro exposure, ozone molecules may have a more direct route to reach cells and interact with their nucleic acids than in an in vivo milieu. Therefore, these positive in vitro results may have little relevance to in vivo exposures.

The results from these leading researchers in the field of adduct detection, although largely negative, provide worthwhile information regarding the effects of ozone on genetic material in the lungs. These findings suggest that the analytic methods may not yet be sensitive enough to detect ozone-induced genetic damage that occurs in vivo. Alternatively, an in vivo ozone exposure simply may not produce these particular adducts. Future refinements of this methodology may improve the sensitivity of these techniques to detect damage to genetic material potentially caused by ozone.

# Localization of Tropoelastin and Type I Procollagen Expression in Lungs After Short-Term Ozone Exposure

*William C. Parks*
*Department of Medicine*
*Jewish Hospital at Washington University Medical Center*
*St. Louis, MO 63110*

## Introduction

Altered connective tissue protein synthesis in the lungs is associated with chronic ozone exposure. However, the specific extracellular matrix components and stromal regions that are affected have not yet been clearly identified. Previous studies have examined alterations in total amounts of collagen and elastin protein content of the lung after ozone exposure (Last et al. 1979, 1984; Costa et al. 1983; Pickrell et al. 1987). Because the extent of ozone damage can vary throughout the lungs, these analytic methods may interfere with an accurate assessment of effects on matrix deposition in the focal areas. This occurs because the total mass of matrix proteins from unaffected areas may obscure detection of matrix alterations from specific areas. To address this problem, we used in situ hybridization to localize sites of gene expression for specific extracellular matrix components in the lungs of normal and ozone-exposed rats.

## Methods

**Tissue Preparation** Rats were exposed for six hours per day, five days per week, to 0 or 1.0 parts per million (ppm) ozone for two months at Batelle Pacific Northwest Laboratories, Richland, WA. The anterior right lobe of each lung was dissected and fixed by intratracheal instillation of 10 percent buffered formalin. Tissues were processed for paraffin embedding and in situ hybridization as described by Prosser and associates (1989). Sections (5 μm) were treated with nuclease-free proteinase K to loosen the constraints of intracellular cross-links and were washed in 0.1 M triethanolamine buffer containing 0.25 percent acetic anhydride to reduce potential nonspecific binding sites.

**In Situ Hybridization** Sections were covered with approximately 25 to 50 μL of hybridization buffer containing 50 percent deionized formamide, twice concentrated standard saline citrate buffer, 20 mM Tris, pH 8.0, standard Denhardt's solution, 1 mM ethylenediaminetetraacetate, 10 percent dextran sulfate, 100 mM dithiothreitol, 0.5 mg/mL yeast tRNA, and 2.5 × 105 cpm of $^{35}$S-labeled antisense or sense RNA. The sections then were incubated at 55°C in a humidified chamber. After hybridization, slides were washed extensively under increasingly stringent conditions, and unbound probe was removed by treatment with RNAase A. Washed slides were dipped in Kodak NTB-2 emulsion and processed for autoradiography. After developing the photographic emulsion, slides were stained with hematoxylin-eosin.

**Probe Preparation** Plasmids containing rat tropoelastin and human α1(I) procollagen cDNA inserts were linearized to transcribe antisense and sense RNAs. Probes were transcribed with α$^{35}$S-labeled uridine triphosphate, as recommended for reagents from Promega (Madison, WI); the reaction was extended to four hours to allow for the relatively inefficient incorporation of sulfated ribonucleotides (Prosser et al. 1989). Unlabeled α-thio uridine triphosphate was added to maintain the total concentration of uridine triphosphate at 15 μM. Under these conditions, RNA of the desired size with specific activities between $10^8$ and $10^9$ dpm/μg were routinely obtained. RNA probes were purified and stored as previously described (Prosser et al. 1989).

## Results

Using established protocols (Parks et al. 1988), probe specificity was confirmed by Northern hybridization of neonatal rat lung RNA with $^{32}$P-labeled RNA probes (data not shown). Because of the pronounced genetic expression of elastin and collagen during fetal development, sections of fetal rat lung served as positive controls for the in situ hybridization procedures (data not shown). As predicted, strong signals for tropoelastin and type I procollagen mRNAs were detected with antisense probes in cells of developing blood vessels and in various stromal compartments on the fetal lung tissue sections. No specific signal was seen in sections incubated with sense RNA probes, indicating the specificity of the antisense probes.

In lung sections from rats exposed to 1.0 ppm ozone for two months, the signal for tropoelastin mRNA was confined to individual cells in many alveoli (Figure 1, lower panels). No signal was detected in alveolar cells in lungs from control rats (Figure 1, upper panels) or in sections hybridized with sense probes. Type I procollagen mRNA was localized in alveolar cells, sites similar to those observed with tropoelastin mRNA (data not shown).

## Discussion

The observations obtained from our pilot study indicate that subchronic ozone exposure induces tropoelastin and procollagen gene expression in alveolar septal cells. Comparing our results with previous findings for elastin and collagen gene expression in ozone-exposed lungs is difficult because the ozone concentrations and treatment protocols differ. In general, ozone exposure mediates small increases in collagen synthesis and deposition (Last et al. 1979, 1984; Myers et al. 1984; Pickrell et al. 1987); one study reported no effect (Wright et al. 1988). The positive findings are consistent with our in situ hybridization data indicating focal expression of type I procollagen in alveolar cells.

Elastin content is typically unchanged or decreased by ozone exposure (Dubick et al. 1981; Costa et al. 1983; Myers et al. 1986; Damji and

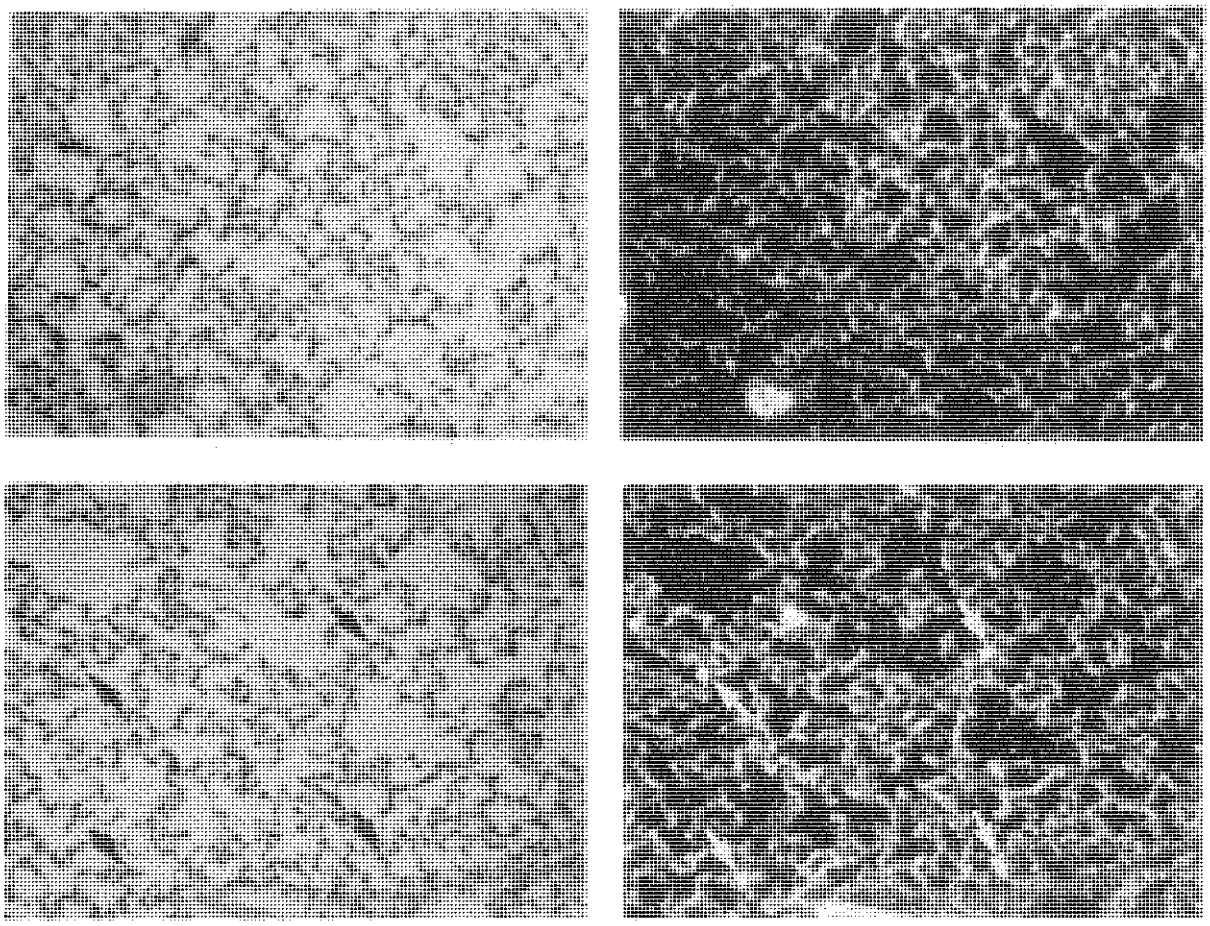

**Figure 1.** In situ hybridization for tropoelastin mRNA in control and ozone exposed rat lung. Lungs from control and ozone-exposed rats (1.0 ppm, two months) were processed for in situ hybridization. Both control and ozone-exposed sections were hybridized with antisense $^{35}S$-labeled RNA specific for tropoelastin mRNA. Autoradiographic exposure was for 10 days. Sections were counterstained with hematoxylin and eosin (magnification × 200). **Upper panels:** paired light (left) and dark (right) field photomicrographs of lung sections from control rats. No specific silver grains were seen. **Lower panels:** paired light and dark field photomicrographs of lung section from ozone-exposed rats. Specific signal for tropoelastin mRNA was detected in individual cells of some alveoli (arrows).

Sherwin 1989), although high doses (2.0 ppm of ozone) can increase elastin content (Costa et al. 1983). The discrepancy between these earlier findings and our observations is not clear. Our in situ hybridization data, however, indicate production of tropoelastin, a precursor of elastin, rather than actual deposition of elastin. The total measured content of lung elastin is a balance between deposition and degradation. Ozone may mediate elastolytic activity and thus account for the decreased elastin content caused by prolonged exposure. The finding that ozone exposure is associated with an inactivation of elastase inhibitors (Johnson 1987) is consistent with this idea. The findings from our studies support the hypothesis that ozone inhalation alters extracellular matrix gene expression. Our future studies using in situ hybridization and immunohistochemistry will provide valuable information regarding alterations in matrix composition caused by ozone exposure.

## References

Costa DL, Kutzman RS, Lehmann JR, Popenoe EA, Drew RT. 1983. A subchronic multidose ozone study in rats. In: International Symposium on the Biomedical Effects of Ozone and Related Photochemical Oxidants (Lee SD, Mustafa MG, Mehlman MA, eds.). Princeton Scientific Publishing Co., Princeton, NJ.

Damji KS, Sherwin RP. 1989. The effect of ozone and simulated high altitude on murine lung elastin: Quantitation by imaging analysis. Toxicol Ind Health 5:995–1003.

Dubick MA, Rucher RB, Last JA, Lollini LO, Cross CE. 1981. Elastin turnover in murine lung after repeated ozone exposure. Toxicol Appl Pharmacol 58:203–210.

Johnson DA. 1987. Effects of Ozone and Nitrogen Dioxide on Human Lung Protease Inhibitors. Research Report Number 11. Health Effects Institute, Cambridge, MA.

Last JA, Greenberg DB, Castleman WL. 1979. Ozone-induced alterations in collagen metabolism of rat lungs. Toxicol Appl Pharmacol 51:247–258.

Last JA, Reiser KM, Tyler WS, Rucker RB. 1984. Long-term consequences of exposure to ozone. Toxicol Appl Pharmacol 72:111–118.

Myers BA, Dubick MA, Gerriets JE, Reiser KM, Last JA, Rucker RB. 1986. Lung collagen and elastin after ozone exposure in vitamin B6–deficient rats. Toxicol Lett 30:55–61.

Myers BA, Dubick MA, Reiser KM, Gerriets JE, Last JA, Rucker RB. 1984. Ozone exposure, food restriction and protein deficiency: Changes in collagen and elastin in rodent lung. Toxicol Lett 23:43–49.

Parks WC, Secrist H, Wu LC, Mecham RP. 1988. Developmental regulation of tropoelastin isoforms. J Biol Chem 263:4416–4423.

Pickrell JA, Hahn FF, Rebar AH, Horoda RA, Henderson RF. 1987. Changes in collagen metabolism and proteinolysis after repeated inhalation exposure to ozone. Exp Mol Pathol 46:400–411.

Prosser IW, Stenmark KR, Suthar M, Crouch EC, Mecham RP, Parks WC. 1989. Regional heterogeneity of elastin and collagen gene expression in intralobar arteries in response to hypoxic pulmonary hypertension as demonstrated by in situ hybridization. Am J Pathol 135:1073–1088.

Wright ES, Kehrer JP, Whiote DM, Smiler KL. 1988. Effects of chronic exposure to ozone on collagen in rat lung. Toxicol Appl Pharmacol 92:445–452.

## Comments

This investigator used in situ hybridization methods to identify changes in the expression of the genetic message for elastin and type I collagen in the lungs of rats after ozone exposure. The rationale for this approach was that it could provide a more sensitive indicator of localized changes in matrix protein production in the alveolar region than conventional whole lung biochemistry.

Sections of fetal rat lung tissue served as positive controls for the specificity of the RNA probes for rat tropoelastin and human type I procollagen mRNA. These sections yielded positive signals for the presence of the genetic message for both of these structural proteins. In subsequent tests, positive signals also were observed for tropoelastin and type I procollagen mRNAs in samples from adult rats exposed to ozone. The increased signal indicated that ozone exposure may have caused increased transcription (formation) of the message, decreased degradation of the message, or both. These findings are consistent with previous biochemical and morphological observations that ozone exposure increases the interstitial matrix content in the lungs of laboratory animals.

In situ hybridization provides site-specific information about regional changes in gene expression in the lungs. However, unlike standard biochemical assays, the results of in situ hybridization are not easily quantified. The figure in the report indicates minimal, patchy signals in the alveolar walls in response to ozone exposure. Future observations, at different ozone exposures and durations and with appropriate controls, could substantiate these preliminary findings. Methods to identify more accurately the particular cell types responsible for the observed signals also would increase the value of this technique.

These preliminary results suggest that further studies may provide new and interesting data related to the effects of ozone on the interstitial matrix of the lungs. Using probes for other matrix components could provide additional insights for the sequence in which genetic messages for matrix proteins are activated in response to ozone exposure. In view of ozone's known effects on alveolar matrix structure, increased mRNA levels for other matrix proteins could be expected.

# Ozone, Extracellular Matrix, and Epithelial Adaptation

*Kent E. Pinkerton and Robert R. Mercer*
*Department of Anatomy*
*University of California at Davis*
*Davis, CA 95616 and*
*Department of Medicine*
*Duke University*
*Durham, NC 27710*

## Introduction

Numerous studies indicate that the effects of ozone are not limited to a single region or specific cell type of the respiratory system (Boorman et al. 1980; Castleman et al. 1980; Eustis et al. 1981; Barry et al. 1985, 1988; Fujinaka et al. 1985; Barr et al. 1988). Injury may be present within all levels of the respiratory system, but the extent of these changes can vary considerably, particularly within the gas exchange region of the lungs (Boorman et al. 1980; Barry et al. 1985; Barr et al. 1988). To better understand these differences, clearly defined sampling strategies were developed to evaluate tissue compartment changes within the lung parenchyma using a simple morphometric approach. These sampling strategies allowed us to analyze the ventilatory unit and to assess more clearly the chronic effects of ozone on the total lung parenchyma. The ventilatory unit, which we define as the basic structural and functional unit of the lungs, comprises the alveolar ventilatory units that include all ducts and alveoli arising from a single terminal bronchiole. All samples for these analyses were taken from the lungs of Sprague-Dawley rats after exposure to 0.98 parts per million (ppm) ozone for eight hours per day for 90 days.

The three specific goals formulated for this pilot study were:

1. to examine parenchymal tissue sampling strategies using large tissue block isolation, en bloc tissue isolation, and serial section analysis;
2. to quantify the structural remodeling of ventilatory units after exposure to ozone using morphometric, serial section, and three-dimensional reconstruction methods; and
3. to compare alveolar wall (i.e., epithelial, interstitial, and vascular compartments) and alveolar septal tip (septal edge) changes as a function of distance from the original bronchiolar-alveolar duct junction within each ventilatory unit.

## Methods

All rats were obtained from Bantin and Kingman (Fremont, CA). Serology, cultures, complete necropsies, and histopathology performed on two randomly selected animals revealed no bacterial or viral infections, pulmonary pathogens, or abnormalities in the tissue structure before exposure. At the onset of exposure, all animals were 65 days old. All rats were maintained in modified 4.2-$m^3$ Hinners-type exposure chambers. The filtered air in the chambers was changed at a rate of 30 times per hour. Temperature was maintained at 24° ± 2°C, and relative

humidity at 40 to 50 percent. Ozone was generated from medical grade oxygen using silent arc discharge ozonizers (model V, Erwin Sander Co., Eltze, Germany). Nocturnal exposure was for eight hours per night (9:00 p.m. to 5:00 a.m.) to 0.98 ± 0.05 ppm ozone (mean ± SD) for a total of 90 days. Ozone concentration was monitored every eight minutes by an ultraviolet ozone monitor (model 1003-AH, Dasibi Environmental Corp., Glendale, CA) calibrated with an absolute ozone photometer (model 1008-PC, Dasibi). Monitoring was controlled and data were recorded by an LSI 1123 computer (Digital Equipment Corp., Maynard, MA). Animals had free access to food and water throughout the study.

Large tissue block isolation was conducted on tissues that had been processed with araldite, embedded in large-face molds, and then sectioned with glass knifes. Terminal bronchiolar-alveolar duct junctions identified on 0.5-μm-thick sections were analyzed using light microscopic morphometry. This approach was simple to perform, but the analysis of tissues was limited to an extremely small region of the lung parenchyma. The extent of these lesions surrounding the bronchiolar-alveolar duct junction could be described as an areal measurement, although extrapolating these measurements to the whole lung was not possible with such a sampling technique. Measurements of value with this approach proved to be step sections through one entire lobe of the lungs for the volume fraction determination of the percentage of the lung parenchyma that underwent histological change.

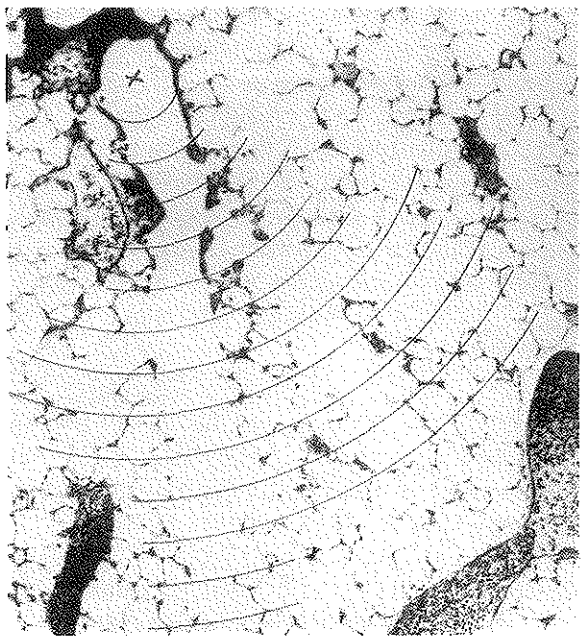

**Figure 1.** Pulmonary acinus isolated with en bloc microdissection approach. Concentric arcs are spaced at 100-μm intervals beginning from the level of the first alveolar outpocketing of the last conducting airway. The reference point from which concentric arcs were drawn is indicated by a small x.

En bloc microdissection was conducted on lung tissue slabs processed with araldite and then embedded in deep wells. These embedded tissue slabs were cut serially into 0.5-mm slices and examined under a dissecting microscope. Terminal bronchiolar-alveolar duct junctions oriented in longitudinal section were identified, isolated, and mounted on blank araldite stubs for sectioning (Figure 1). Longitudinal cuts were taken through terminal bronchioles so that the cuts bisected the first alveolar duct bifurcation and its adjacent pair of alveolar ducts. We recognized that this sampling approach provided us with the same orientation as the path of a gas molecule traveling through the ventilatory unit. This observation led us to decide that the most logical approach for evaluating changes in the ventilatory unit was to identify a reference point at or near the junction of the terminal bronchiole and alveolar duct. From this point, we could draw concentric arcs through this two-dimensional profile and measure changes as a function of distance from the reference point.

Three-dimensional reconstruction of ventilatory units was done in the right cranial lung lobe that had been embedded in paraffin and then serially sectioned. A computer program designed for these reconstructions was used to generate images. Changes in the lungs were evaluated by mathematical data analysis from these same three-dimensional images (Mercer and Crapo 1989; Mercer et al. 1991). Surface areas, volumes, and the mean caliper diameter of the ventilatory unit were measured. Serial section analysis also was used to determine the percentage of the ventilatory unit that showed histologic change as a result of ozone exposure. These three-dimensional measurements were compared with data from single sections of ventilatory units that had been isolated with either the large block or en bloc microdissection technique.

## Results

An example of a ventilatory unit isolated by the en bloc microdissection approach is shown in Figure 1. Alveolar septal tips were distinguished

**Table 1. Microdosimetry Analysis[a]**

| Distance (mm) | Alveolar Wall (μm) Control | Alveolar Wall (μm) Exposed | Septal Tip (μm) Control | Septal Tip (μm) Exposed | Predicted Dose (%) |
|---|---|---|---|---|---|
| 0–0.2 | 5.6 ± 1.1 | 13.6 ± 2.6[b] | 11.6 ± 1.6 | 19.6 ± 2.0[b] | 100.0 |
| 0.2–0.4 | 5.9 ± 1.1 | 10.9 ± 2.7[b] | 12.3 ± 1.8 | 22.2 ± 1.9[b] | 42.0 |
| 0.4–0.6 | 5.1 ± 0.3 | 7.1 ± 0.7[b] | 8.6 ± 1.2 | 18.1 ± 1.5[b] | 14.0 |
| 0.6–0.8 | 5.1 ± 0.5 | 6.0 ± 0.4 | 8.3 ± 0.9 | 10.8 ± 1.8 | 5.6 |
| 0.8–1.0 | 5.2 ± 0.5 | 5.5 ± 0.6 | 8.8 ± 1.0 | 9.6 ± 1.0 | 0.2 |

[a]All measurements are mean ± SE; $n = 4$ animals.
[b]Significantly different from control ($p < 0.05$) by Duncan's multiple comparison test.

from alveolar walls by drawing an imaginary line that separated alveolar air spaces from the alveolar duct lumen. All tissues that touched this line were considered part of the alveolar septal tip, which is the mouth opening of each alveolus to the alveolar duct. This method provided a simple way of separating these two structures without introducing subjective bias on the part of the observer.

Four to five ventilatory units were isolated from each animal. Each ventilatory unit then was photographed and printed on 11- by 14-inch paper. Concentric arcs were drawn at 100-μm intervals from a reference point situated at the level of the first alveolar outpocketing along the terminal bronchiolar airway wall. Only those arc lengths that intercepted a bronchiolar wall, septal tip, or alveolar wall of an alveolus that opened onto a duct in direct communication with a bronchiolar-alveolar duct junction were measured. Each intercept was viewed directly under the microscope and its length recorded using a 20- by 20-inch Numonics (Montgomeryville, PA) 2000 digitizing tablet and a cursor with a pinpoint light source. A photoextension tube on the microscope permitted us to see the light source and directly measure the intercept length with a higher degree of resolution than that possible with the "arc map" used to identify points for analysis.

Measurements from the four to five ventilatory units were arranged to represent one animal. Table 1 provides a summary of the data from four animals of the average measurements recorded for

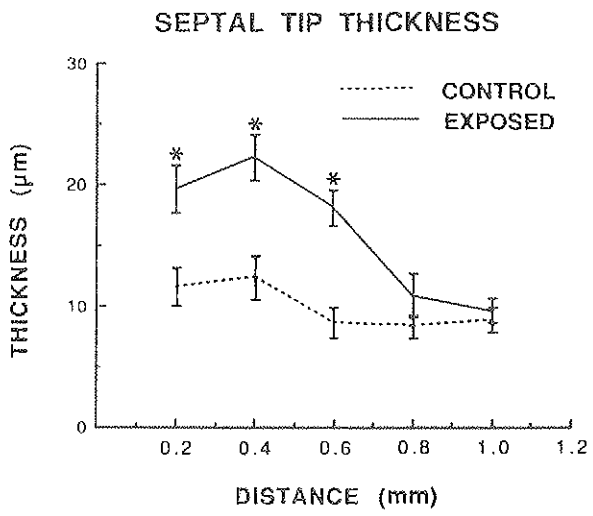


**Figure 2.** Septal tip (edge) thickness expressed as a function of distance into the pulmonary acinus from the bronchiolar-alveolar duct junction in the lungs of animals exposed to ozone or to filtered air (control). An * indicates a value significantly different from control ($p < 0.05$) by Duncan's multiple comparison test.

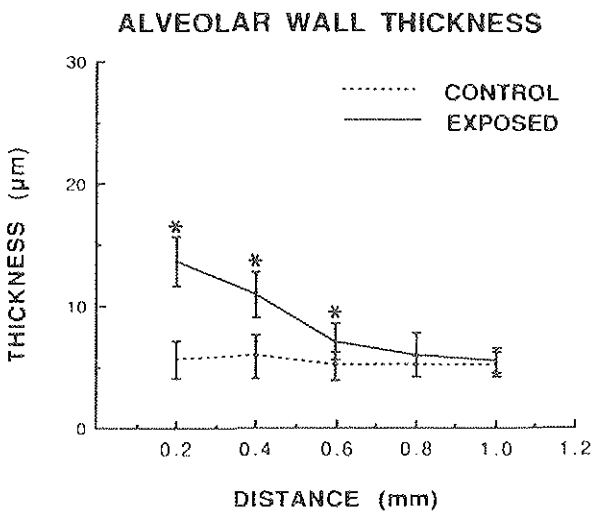


**Figure 3.** Alveolar septal wall thickness expressed as a function of distance into the pulmonary acinus from the bronchiolar-alveolar duct junction in the lungs of animals exposed to ozone or to filtered air (control). An * indicates a value significantly different from control ($p < 0.05$) by Duncan's multiple comparison test.

the thickness of alveolar walls and septal tips along the ventilatory unit for control and ozone-exposed animals. This table includes predictions for decreases in the percentage of initial ozone dose present at the bronchiolar-alveolar junction as it penetrates into selected depths of the ventilatory unit. These predictions are based on the mathematical model derived by Mercer and colleagues (Mercer and Crapo 1989; Mercer et al. 1991). There was a significant increase in alveolar wall thickness and in the thickness of the septal tip (also referred to as the septal edge) subcompartment of the alveolar septa. For both of these measurements, the tissue response to ozone was limited to the first 0.6-mm region of the ventilatory unit. The measured tissue response versus the distance from entry into the ventilatory unit was comparable to that predicted by the dosimetry model for the distribution of ozone uptake by the ventilatory unit (Table 1).

Figures 2 and 3 illustrate the changes in the thickness of the alveolar septal wall and alveolar septal tip (edge) as a function of distance from the bronchiolar-alveolar duct junction. The thickness of the alveolar wall in the first 100 μm from the bronchiolar-alveolar duct junction of exposed animals (solid line) increased 140 percent compared with the corresponding control value (dashed line). This thickening resulted predominately from replacement of the squamous Type 1 epithelium of the alveolar spaces with a mixture of cuboidal epithelium and extended from the airway epithelium into the alveolar region.

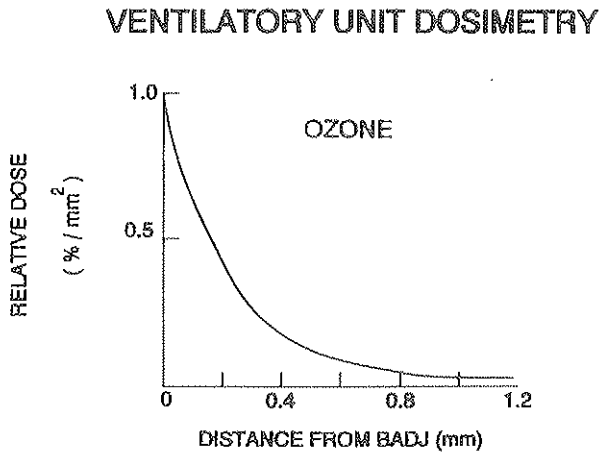


**Figure 4.** Ozone uptake in the pulmonary acinus predicted by a mathematical model of ventilatory unit dosimetry. An estimated 90% of the initial ozone dose was taken up approximately 0.5 mm from the site of the bronchiolar-alveolar duct junction (BADJ).

Predictions of estimated ozone uptake in the ventilatory unit derived from mathematical models (Overton 1984; Miller et al. 1985; Mercer et al. 1991) are shown in Figure 4. Uptake along the ventilatory unit was almost 90 percent of the initial value at a distance of approximately 0.5 mm. In measurements of ventilatory unit response to ozone, significant alterations in alveolar wall thickness and septal edge thickness were observed in the first 0.6 mm.

## Discussion

The findings from our pilot study demonstrate the utility of tissue sampling strategies that exploit the relationship between the structural units of the lung and their basic functional properties. In our study, we took complete advantage of the fact that the ventilatory unit is not only a distinct structural entity, but also the basic unit of gas exchange in the lung parenchyma. We combined use of en bloc microdissection methods, concentric arc measurements from a defined reference point, and three-dimensional analysis of the ventilatory unit to test the principles of ozone microdosimetry in the lungs. This combination of powerful tools will help us to understand better the heterogeneous nature of ozone-induced injury in the lung parenchyma.

## References

Barr BC, Hyde DM, Plopper CG, Dungworth DL. 1988. Distal airway remodeling in rats chronically exposed to ozone. Am Rev Respir Dis 137:924–938.

Barry BE, Mercer RR, Crapo JD. 1988. Effects of inhalation of 0.25 ppm ozone on the terminal bronchioles of juvenile and adult rats. Exp Lung Res 14:225–245.

Barry BE, Miller FJ, Crapo, JD. 1985. Effects of inhalation of 0.12 and 0.25 parts per million ozone on the proximal alveolar region of juvenile and adult rats. Lab Invest 53:692–704.

Boorman GA, Schwartz LW, Dungworth DL. 1980. Pulmonary effect of prolonged ozone insult in rats: Morphometric evaluation of the central acinus. Lab Invest 43:108–115.

Castleman WL, Dungworth DL, Schwartz LW, Tyler WS. 1980. Acute respiratory bronchiolitis: An ultrastructural and autoradiographic study of epithelial cell injury and renewal in rhesus monkeys exposed to ozone. Am J Pathol 98:811–840.

Eustis SL, Schwartz LW, Kosch PC, Dungworth DL. 1981. Chronic bronchiolitis in nonhuman primates

after prolonged ozone exposure. Am J Pathol 105:121–137.

Fujinaka LE, Hyde DM, Plopper CG, Tyler WS, Dungworth DL, Lollini LO. 1985. Respiratory bronchiolitis following long-term ozone exposure in bonnet monkeys: A morphometric study. Exp Lung Res 8:167–190.

Mercer RR, Anjilvel S, Miller FJ, Crapo JD. 1991. Inhomogeneity of ventilatory unit volume and its effects on reactive gas uptake. J Appl Physiol 70:2193–2205.

Mercer RR, Crapo JD. 1989. Anatomical modeling of microdosimetry of inhaled particles and gases in the lung. In: Extrapolation of Dosimetric Relationships for Inhaled Particles and Gases (Crapo JD, Smolko ED, Miller FJ, Graham JA, Hayes AW, eds.) pp. 69–78. Academic Press, Orlando, FL.

Miller FJ, Overton JH, Jaskot RH, Menzel DB. 1985. A model of the regional uptake of gaseous pollutants in the lung: I. The sensitivity of the uptake of ozone in the human lung to lower respiratory tract secretions and exercise. Toxicol Appl Pharmacol 79:11–27.

Overton JH. 1984. Physicochemical processes and the formulation of dosimetry models. J Toxicol Environ Health 13:274–298.

## NIEHS COMMENTARY

The aim of this study was to develop morphometric techniques for quantifying ozone-induced changes in the pulmonary acinus, which is the basic structural and functional unit for gas exchange in the lungs. The investigators selected lung tissue samples from groups of four rats exposed either to 1 ppm ozone or air for 90 days. They then tested whether the extent of structural changes decreased with increasing distance from the junction in the acinus between the terminal bronchiole and the alveoli that emanate from it.

The investigators used photographs of serial sections cut through pulmonary acini, three-dimensional computer-generated reconstructions of the acini, and a newly-designed photograph overlay to measure the alterations in the thickness of the alveolar walls and septal tips caused by ozone exposure. Alveolar walls and septal tips of tissue from the animals exposed to ozone were approximately twice as thick as those measured on control samples. Thickness decreased with distance from the bronchiolar-alveolar duct junction, and few changes were evident beyond 0.6 mm. These findings correlated well with the dosimetric prediction that more than 90 percent of the ozone uptake occurs within 0.5 mm of the junction.

This study attests to the capability of ultrastructural morphometric techniques to detect subtle changes in lung tissue caused by ozone. Although these preliminary data were based on a small number of observations, they were consistent with previous data regarding the fibrotic responses of lung tissue to ozone exposure. The extent of tissue damage also correlated well with the author's model of ozone dosimetry within the acini. It will be interesting to apply these methods to lung samples obtained after longer exposures to ozone and correlate these data with biochemical and physiological data.

# Assessment of Airway Responsiveness to Inhaled Methacholine and the Effects of Short-Term Ozone Exposure in Aged Fischer-344 Rats

*Derek A. Uchida, Clark A. Ballowe, Charles G. Irvin, and Gary L. Larsen*
*National Jewish Center for Immunology and Respiratory Medicine*
*Denver, CO 80206*

## Introduction

Short-term exposure to ozone results in airway hyperresponsiveness in animals and humans (Golden et al. 1978; Holtzman et al. 1983; Murlas and Roum 1985; Evans et al. 1988). Few data have been gathered on the effect of chronic ozone exposure on airway responsiveness. Airway hyperresponsiveness correlates with the severity of asthmatic symptoms and with medication requirements in both adults (Juniper et al. 1981) and children (Murray et al. 1981). Measuring this important parameter of airway function in the National Toxicology Program (NTP)/Health Effects Institute (HEI) chronic ozone exposure study animals when they become available may provide clues to the relationship between chronic exposure to ambient levels of ozone and respiratory diseases such as asthma. Our intentions in this pilot project were (1) to refine the techniques of measuring lung function and airway responsiveness to both inhaled and intravenous methacholine in rats similar in age and species to those used in the NTP/HEI chronic ozone exposure study; and (2) to examine the effects of short-term ozone exposure (1 part per million [ppm] for four hours) on airway responsiveness in these animals.

## Methods

Twelve-month-old Fischer-344 rats were used in this study. The animals were anesthetized and orally intubated. All measurements of pulmonary function were made with the animals breathing spontaneously. A saline-filled catheter attached to a transducer was placed in the esophagus and positioned so that maximal negative pressure deflections were obtained from the inspiratory efforts of the animals. A pressure plethysmograph was used and tidal volume changes were monitored with a differential pressure transducer. The plethysmograph was connected directly to a chamber filled with copper gauze that served as a heat sink. The negative port of the transducer was referenced to a second chamber filled with copper gauze. This second chamber was connected to the first chamber with PE 205 polyethylene tubing. The time constant of this tubing was long enough to stabilize the changes in the volume signal against thermal drift. Pressure and volume signals were fed into an analog computer that calculated pulmonary resistance ($R_L$) based on techniques described by Amdur and Mead (1958). Pressure, volume, flow (derived from differentiation of the volume signal), and minute ventilation were also monitored and recorded throughout the experiments.

Inhalational challenge with methacholine was accomplished by using an ultrasonic nebulizer to generate a mist of methacholine and delivering it to the animal at a constant flow of 250 mL/minute, via a t-piece adaptor attached to the endotracheal tube. Each animal first received a nebulized dose of saline for 15 seconds, and the baseline value for $R_L$ was recorded after saline inhalation. Nebulized methacholine then was delivered in doubling dose concentrations of 0.075, 0.15, 0.3, 0.6, 1.25, 2.5, and 5.0 mg/mL. Each animal was exposed to each dose for 15 seconds, and pulmonary function was then measured during the subsequent two minutes, or until $R_L$ peaked. Once $R_L$ achieved a value that was 150 percent of the saline baseline value, delivery of further methacholine doses was terminated. Methacholine dose-response curves were generated by plotting the concentration of methacholine delivered on the x axis (log scale) against $R_L$ as a percentage of the saline baseline value on the y axis (linear scale). Airway responsiveness was expressed as the concentration of methacholine needed to provoke an increase in $R_L$ to 150 percent of the saline baseline value ($PC_{150}R_L$). Thus, a decrease in $PC_{150}R_L$ represented an increase in airway responsiveness because it indicated that less methacholine was needed to reach the 150 percent target value. Prior to any ozone exposure, baseline curves were obtained for the animals' responsiveness to the methacholine dose series. Two to four days later, animals were exposed to 1 ppm ozone for four hours. Airway responsiveness to the same methacholine dose series then was reassessed one hour after ozone exposure.

An intravenous methacholine challenge was performed by anesthetizing an animal and applying a tourniquet to the base of its tail. A 27-gauge needle then was inserted into a tail vein and secured in place. The needle was attached to a syringe pump and doubling doses of methacholine (0.6, 1.2, 2.3, 4.5, 8.7, and 17 mg/minute) were infused sequentially while pulmonary function was monitored. Two days after the baseline intravenous methacholine challenge, animals were exposed to 2 ppm ozone for four hours. Airway responsiveness to intravenous methacholine was reassessed one hour after ozone exposure.

Results are expressed as the mean ± SEM. Statistical analyses were performed using the Student's paired or unpaired *t* test. Statistical significance was defined as a *p* value that was less than 0.05.

## Results

Figure 1 shows the effect of ozone exposure on airway responsiveness to inhaled methacholine in seven animals. Exposure to ozone at 1 ppm for four hours resulted in a significant increase (Student's paired *t* test, $p < 0.05$) in airway responsiveness to inhaled methacholine. This effect was indicated by a significant decrease in $PC_{150}R_L$. In contrast, four animals exposed to room air under the same conditions showed no change in airway responsiveness (Figure 1). Measurements of airway responsiveness to inhaled methacholine in Fischer rats demonstrated a moderate amount of interanimal variability (Figure 2, "no treatment" group). However, as a group, animals exposed to ozone were significantly more responsive to inhaled methacholine than animals not exposed to ozone (Student's unpaired *t* test, $p < 0.05$). Minute ventilation for animals studied on different days was not significantly different within the control and experimental groups (data not shown).

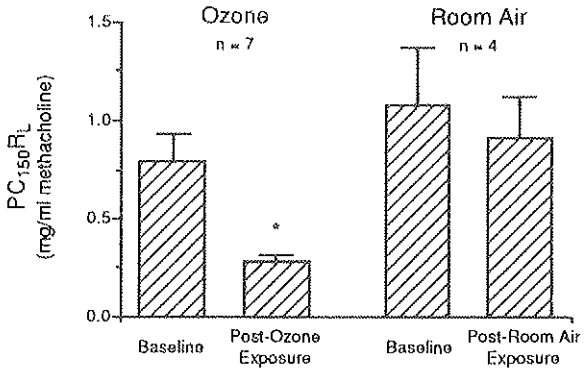


**Figure 1.** Airway responsiveness to inhaled methacholine at baseline and after exposure to ozone or room air. Exposure to ozone resulted in a significant increase in airway responsiveness, whereas room air had no effect. An * indicates a statistical significance value of $p < 0.05$.

At the light microscopic level, no detectable differences were observed in the structure of the airways from a rat exposed to ozone and then challenged with inhaled methacholine, compared with the airways of a rat exposed to ozone alone.

An intravenous methacholine challenge was performed on two animals before and after ozone exposure. Ozone exposure did not change airway responsiveness to intravenous challenge in either animal (Figure 3).

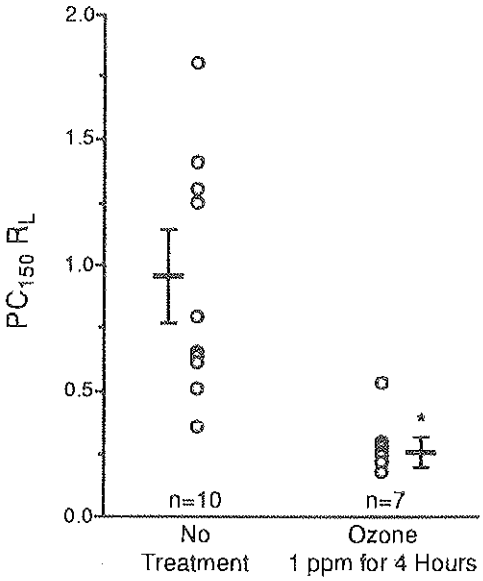


**Figure 2.** Values of $PC_{150}R_L$ for individual animals before exposure to ozone (no treatment) and after exposure to 1 ppm ozone for four hours. Twelve-month-old Fischer-344 rats displayed a moderate amount of interanimal variability, as evidenced by the wide scatter in $PC_{150}R_L$ within the no-treatment group. This group did not receive a sham exposure with air prior to ozone exposure. After ozone exposure, the variability was reduced and airway responsiveness was significantly higher than that for the no-treatment group (as measured by Student's unpaired *t* test). An * indicates a statistical significance value of $p < 0.05$. Error bars indicate SEM.

## Discussion

In this pilot study, we have shown that airway responsiveness to inhaled and intravenous methacholine can be measured on anesthetized, spontaneously breathing, 12-month-old Fischer-344 rats. Exposure of these rats to ozone (1 ppm for four hours) resulted in a significant increase in airway responsiveness to inhaled methacholine one hour after exposure. Although it is impossible to predict accurately from short-term exposure studies whether chronic exposure to higher levels of ozone would have the same effect on airway responsiveness, these results raise significant questions about the health effects of chronic exposure. As stated earlier, the measurement of this important parameter of airway function has relevance for the NTP/HEI chronic ozone exposure study. In that study, measurements of airway responsiveness in the same animals before and after exposure will not be possible. Therefore, comparisons must be made between a group of animals exposed to ozone and a separate control group of animals not exposed to ozone. This could make detecting differences between experimental and control groups difficult, because, as in humans, airway responsiveness in Fischer-344 rats appears to demonstrate a moderate amount of interanimal variability. However, in this pilot study, the animals exposed to ozone were, as a group, significantly more responsive than animals not exposed to ozone (Figure 3). Hence, we do not anticipate that interanimal variability will be a problem in interpreting the results from the NTP/HEI chronic ozone exposure study.

The techniques used in this study for the inhaled methacholine challenge procedure did not seem to alter the structure of the lungs based on our light microscopic evaluations of tissue samples. This is consistent with our previous experience with a large number of Sprague-Dawley rats that had undergone the same procedures (D.A. Uchida, unpublished observations). However, light microscopy is a relatively insensitive measure of subtle histological changes. Methacholine exposure and subsequent bronchoconstriction may lead to subtle changes in lung histology that would only be recognized using more sensitive methods of tissue analysis, such as those being planned for use on the animals from the NTP/HEI chronic ozone exposure study. Dedicating a group of animals for the sole purpose of respiratory physiological assessment would alleviate these concerns.

Airway responsiveness to intravenous methacholine was not changed by ozone exposure in the two animals studied. Similar discrepancies between inhaled and intravenous challenges after ozone exposure have been documented in a canine model (Bethel and McClure 1991). A plausible explanation for these differences is that short-term exposure to ozone in these animals primarily affects the permeability of the epithelial barrier. It is possible that short-term exposure to ozone increases the permeability of the airway epithelium. If true, this may allow for enhanced delivery of inhaled (but not intravenous) methacholine to sites of action such as airway smooth muscle, resulting in airway hyperresponsiveness. In contrast, studies performed using other species have shown increased airway responsiveness to intravenous agonists after ozone exposure (Murlas and Roum 1985). Thus, under certain conditions, ozone exposure may stimulate mechanisms other than a change in epithelial permeability, which results in increased smooth muscle contractility. The NTP/HEI chronic ozone exposure study may shed new light on these mechanisms linking ozone and airway responses.

## References

Amdur MO, Mead J. 1958. Mechanics of respiration in unanesthetized guinea pigs. Am J Physiol 192:364–368.

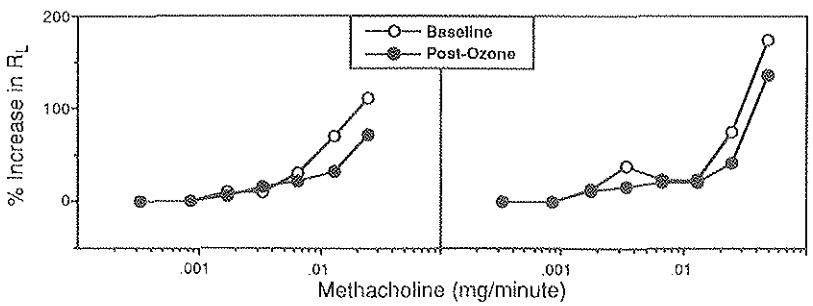


**Figure 3.** Data from two animals that received intravenous methacholine challenges before (open circles) and after (filled circles) ozone exposure. In contrast to the findings using inhaled methacholine challenge, airway responsiveness to intravenous methacholine was unchanged by exposure to ozone.

Bethel RA, McClure CL. 1990. Differential effect of ozone on the response of canine airways to nebulized and parenteral acetylcholine. Am Rev Respir Dis 141:A658.

Evans TW, Brokaw JJ, Chung KF, Nadel JA, McDonald DM. 1988. Ozone-induced bronchial hyperresponsiveness in the rat is not accompanied by neutrophil influx or increased vascular permeability in the trachea. Am Rev Respir Dis 138:140–144.

Golden JA, Nadel JA, Boushey HA. 1978. Bronchial hyperirritability in healthy subjects after exposure to ozone. Am Rev Respir Dis 118:287–294.

Holtzman MJ, Fabbri LM, O'Byrne PM, Gold BD, Aizawa H, Walters EH, Alpert SE, Nadel JA. 1983. Importance of airway inflammation for hyperresponsiveness induced by ozone. Am Rev Respir Dis 127:686–690.

Juniper EF, Frith PA, Hargreave FE. 1981. Airway responsiveness to histamine and methacholine: Relationship to minimum treatment to control symptoms of asthma. Thorax 36:575–579.

Murlas CG, Roum JH. 1985. Sequence of pathologic changes in the airway mucosa of guinea pigs during ozone-induced bronchial hyperreactivity. Am Rev Respir Dis 131:314–320.

Murray AB, Ferguson AC, Morrison B. 1981. Airway responsiveness to histamine as a test to overall severity of asthma in children. J Allergy Clin Immunol 68: 119–124.

## A B S T R A C T

The purpose of this study was to refine methods for measuring airway responsiveness in rats caused by chronic ozone exposure. The primary aim was to evaluate the feasibility of these methods for rats that are aged, potentially sick, and may have significantly compromised respiratory systems.

The investigators successfully developed procedures for both aerosolized and intravenous delivery of methacholine, a drug that causes airway constriction. They then measured pulmonary resistance in one-year-old rats after ozone exposure using both drug delivery routes.

Confirming the work of others, they reported that a four-hour exposure to 1 ppm ozone increased the tendency for airway constriction after treatment with aerosolized methacholine. Animals exposed to ozone needed one-third as much methacholine to elicit the same degree of airway constriction as that needed by control animals exposed to air. Before ozone exposure, the aged rats exhibited wide variations in the amount of methacholine that was required to produce a target level of airway responsiveness. However, ozone exposure reduced this variability and significantly decreased the required amounts of methacholine.

In contrast, intravenous delivery of methacholine produced no changes in airway responsiveness after ozone exposure. This finding suggests that an increase in airway epithelial permeability caused by ozone exposure may mediate an airway responsiveness to aerosolized methachaline that cannot be elicited by intravenous delivery. The reported effects of these acute exposures in aged rats may relate to the effects of ozone expasure in adults with asthma and other respiratory diseases.

# Quantitative Ultrastructural Analysis of Connective Tissue in the Lungs

*Renaud Vincent, Robert R. Mercer, Ling-Yi L. Chang, Frederick J. Miller, Daniel L. Costa, and James D. Crapo*
*Duke University Medical Center*
*Durham, NC 27710 and*
*Health Effects Research Laboratory*
*U.S. Environmental Protection Agency*
*Research Triangle Park, NC 27711*

## Introduction

Inhalation of ozone ($O_3$) and nitrogen dioxide ($NO_2$) can induce fibrosis and emphysema-like lesions in the lungs of laboratory animals. It is, therefore, conceivable that subtle morphologic changes caused by photochemical oxidants could precipitate or predispose susceptible human populations to lung disorders (U.S. Environmental Protection Agency 1986). Animal studies have established that ambient to near-ambient levels of oxidants produce lesions in the centriacinar region of the lungs, as evidenced by cellular injuries, hyperplastic and hypertrophic changes, inflammation, and thickening of the interstitium (Boorman et al. 1980; Barry et al. 1985, 1988; Chang et al. 1986, 1988). The question remains whether these injuries and inflammatory events recur during prolonged ozone exposure and result in fibroblast activation (Goldstein and Fine 1986; Schraufnagel et al. 1987). Such responses may stimulate progressive changes in matrix components, such as an abnormal accumulation of collagen in the central acinus (Last et al. 1979, 1984; Pickrell et al. 1987; Reiser et al. 1987; Tyler et al. 1988).

Several studies have shown the potential of stereological methods to quantify tissue components and to provide sensitive indices of biological effects in these components. The objective of this pilot study was to obtain, by quantitative analysis at the electron microscope level, ultrastructural evidence of matrix alterations within the alveolar tissue immediately distal to the terminal bronchioles in the lungs of rats chronically exposed to ambient or near-ambient concentrations of $O_3$ and $NO_2$.

## Methods

Fischer-344 rats (males, six weeks of age at the start of treatment, specific pathogen free), were exposed for 18 months to separate urban patterns of $O_3$ and $NO_2$. These exposures were performed as part of a collaborative study between the Center for Extrapolation Modeling at Duke University Medical Center and the U.S. Environmental Protection Agency in Research Triangle Park, NC. A detailed description of the exposure facility and exposure patterns is available elsewhere (Davies et al. 1987). The $O_3$ exposure consisted of a background level of 0.06 parts per million (ppm) for 13 hours, an exposure spike peaking at 0.25 ppm over nine hours (equivalent to a nine-hour square-wave exposure averaging 0.19 ppm), and a downtime of two hours for servicing the facility. The $NO_2$ exposure consisted of a 0.5-ppm background level for 16 hours, an exposure spike for six hours, and a two-hour downtime for service. The exposure spike was a one-hour rise to a concentration of 1.2 ppm $NO_2$ followed by a second-hour rise to 1.5 ppm. Exposure was maintained at 1.5 ppm for two hours and returned to the background level over a two-hour period. Weekend exposures for both gases were at the background level. The lung samples analyzed in the following experiments were obtained from animals that were killed (1) immediately after the interruption of exposures; and (2) after a four-month recovery period in clean air, in order to assess the reversibility of the morphological changes.

Sections of alveolar tissue that contained the first generation of alveolar ducts adjacent to a terminal bronchiole (called the proximal alveolar region) were cut perpendicular to the axis of the bronchiole (Barry et al. 1985; Chang et al. 1986). Three sites from each of 12 animals in each group were analyzed. Ultrathin sections were stained with tannic acid by the method described by Kageyama and coworkers (1984), and then stained with uranyl acetate and lead citrate. The interstitial matrix was subdivided into four compartments: collagen fibers, elastin fibers, basement membranes (which combined both epithelial and endothelial basement membranes), and the remaining acellular space or ground substance. Morphometric analyses were performed by point-counting on 11- × 14-inch prints at a final magnification of × 8,500, using an overlay with 112 2-cm lines and 224 points (Weibel 1979; Barry et al. 1985; Chang et al. 1986). Results were calculated as the ratio of the volume density of matrix components to the surface density of epithelial basement membrane, and the final unit of measure was expressed in micrometers.

**Table 1. Volume Densities of the Interstitium Components Normalized Over Epithelial Basement Membrane Surface for Control Animals[a]**

| | 18-Month Exposure Group | 4-Month Recovery Group |
|---|---|---|
| Acellular space | 0.069 ± 0.006 | 0.079 ± 0.006 |
| Elastic fibers | 0.014 ± 0.003 | 0.014 ± 0.001 |
| Collagen fibers | 0.117 ± 0.010 | 0.152 ± 0.012 |
| Basement membranes | 0.108 ± 0.007 | 0.135 ± 0.006 |
| Total matrix | 0.309 ± 0.018 | 0.380 ± 0.016 |
| Interstitial cells | 0.130 ± 0.010 | 0.169 ± 0.017 |
| Interstitium | 0.438 ± 0.026 | 0.549 ± 0.029 |

[a]Values are Mean ± SE given in micrometers; $n = 12$.

## Results

The results of analyses performed on tissue sections from control animals exposed to air are summarized in Table 1. Chronic inhalation of the oxidants produced shifts in the volume densities of interstitial matrix components (Figure 1). Exposure to $O_3$ for 18 months produced significant increases in the amounts of collagen fibers (42 percent) and basement membranes (59 percent) in the proximal alveolar region (Figure 1a). Elevation of collagen volume density was associated with a statistically significant increase in the volume density of interstitial cells (26 percent). This effect was not observed in the animals exposed to $NO_2$. Nitrogen dioxide exposure produced a significant increase in the acellular space (43 percent). Elastin fiber volume density was slightly depressed, but not significantly (17 percent).

Changes in the animals exposed to $O_3$ persisted after recovery in clean air for four months; acellular space, collagen fibers, and basement membranes were all elevated (Figure 1b). Damage to collagen fibers and interstitial edema were considered as possible factors that may have accounted for the increased volume density of collagen fibers; a looser association of the collagen fibrils could have produced an apparently higher volume density of fibers in tissue without an actual increase in collagen mass. However, upon analysis, no difference was detected in the volume density of fibrils within collagen fibers between the control and ozone-exposed groups at 18 months of exposure (determined on prints at magnification of × 14,000; data not shown). Therefore, the increase in the volume density of the collagen fiber compartment detected in the animals exposed to

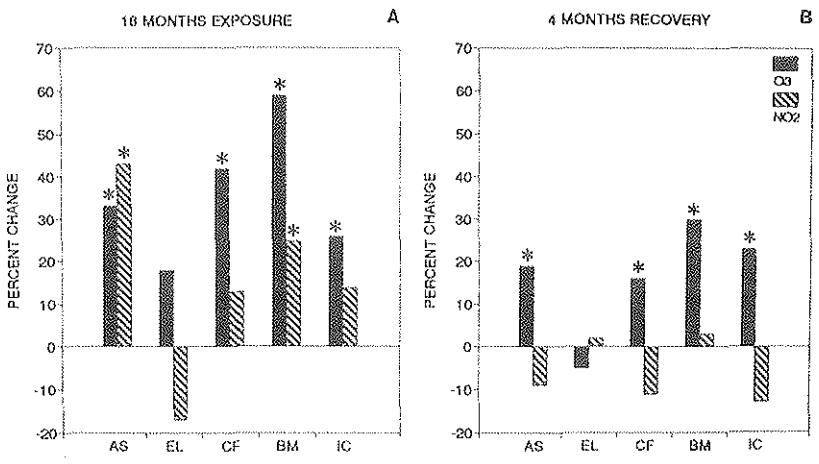


**Figure 1.** Mean percentage of change in the normalized volume density of interstitial matrix components relative to air controls after oxidant treatment and recovery in clean air. Two-way multivariate analysis of variance (ANOVA) techniques, including testing with single- degree-of-freedom contrasts, were used to analyze the raw data. The significance is representative of the effects found by multivariate ANOVA (an * indicates $p < 0.05$). AS = acellular space; EL = elastin fibers; CF = collagen fibers; BM = basement membranes; IC = interstitial cells.

$O_3$ after 18 months of exposure appears to be the result of an accumulation of mature, cross-linked collagenous material.

## Discussion

This study directly addressed the complex issue of identifying subtle adverse effects of chronic exposure to air pollutants. This issue has substantial importance to the national public health. We hypothesized that, if the toxic effects of low concentrations of $O_3$ and $NO_2$ are analogous to those that occur at high doses, these effects should be reflected in changes in interstitial matrix components in the centriacinar region. However, small, focal increases in collagen deposition and alterations of elastin in the lungs cannot be quantified reliably with standard biochemical and histological methods. We evaluated the feasibility of electron microscopic stereological measurements for quantifying changes in interstitial matrix components that occur at focal injury sites in the lungs. The results convincingly demonstrate changes in interstitial matrix components with oxidant exposure. In particular, we see a net accumulation of collagen in animals exposed to $O_3$.

Collagen and elastin repair and synthesis may be affected by different classes of fibroblasts and be regulated by different mechanisms. Of significant interest is the possible change in the volume density of elastin fibers, which could have resulted from an increased turnover of elastin. However, a high variance for elastin measurements precludes definitive conclusions. This variance seems related in part to the heterogeneous distribution of elastin in alveolar duct walls of rats (Mercer and Crapo 1990). It is, therefore, essential to design an improved sampling strategy that allows more accurate measurements of the shifts in the elastin fiber content and distribution.

The research described in this article has been reviewed by the Health Effects Research Laboratory, U.S. Environmental Protection Agency, and approved for publication. Approval does not signify that the contents necessarily reflect the views and policies of the Agency, nor does mention of trade names or commercial products constitute endorsement or recommendation for use.

## References

Barry BE, Mercer RR, Miller FJ, Crapo JD. 1988. Effects of inhalation of 0.25 ppm ozone on the terminal bronchioles of juvenile and adult rats. Exp Lung Res 14:225–245.

Barry BE, Miller FJ, Crapo JD. 1985. Effects of inhalation of 0.12 and 0.25 parts per million ozone on the proximal alveolar region of juvenile and adult rats. Lab Invest 53:692–704.

Boorman GA, Schwartz LW, Dungworth DL. 1980. Pulmonary effects of prolonged ozone insult in rats. Morphometric evaluation of the central acinus. Lab Invest 43:108–115.

Chang LY, Graham JA, Miller FJ, Ospital JJ, Crapo JD. 1986. Effects of subchronic inhalation of low concentrations of nitrogen dioxide: I. The proximal alveolar region of juvenile and adult rats. Toxicol Appl Pharmacol 83:46–61.

Chang LY, Mercer RR, Stockstill BL, Miller FJ, Graham JA, Ospital JJ, Crapo JD. 1988. Effects of low levels of $NO_2$ on terminal bronchiolar cells and its relative toxicity compared to $O_3$. Toxicol Appl Pharmacol 96:451–464.

Davies DW, Walsh LC III, Hiteshew ME, Ménache MG, Miller FJ, Grose EC. 1987. Evaluating the toxicity of oxidant gases: I. An automated chronic gaseous animal inhalation exposure facility. J Toxicol Environ Health 21:89–97.

Goldstein RH, Fine A. 1986. Fibrotic reactions in the lung: The activation of the lung fibroblast. Exp Lung Res 11:245–261.

Kageyama M, Takagi M, Parmley RT, Toda M, Hirayama H, Toda Y. 1984. Ultrastructural visualization of elastic fibers with a tannate-metal salt method. Histochem J 17:93–103.

Last JA, Greenberg DB, Castleman WL. 1979. Ozone-induced alterations in collagen metabolism of rat lungs. Toxicol Appl Pharmacol 51:247–258.

Last JA, Reiser KM, Tyler WS, Rucker RB. 1984. Long-term consequences of exposure to ozone: I. Lung collagen content. Toxicol Appl Pharmacol 72:111–118.

Mercer RR, Crapo JD. 1990. Spatial distribution of collagen and elastin fibers in the lungs. J Appl Physiol 69:756–765.

Pickrell JA, Hahn FF, Rebar AH, Horoda RA, Henderson RF. 1987. Changes in collagen metabolism and proteinolysis after repeated inhalation exposure to ozone. Exp Mol Pathol 46:159–167.

Reiser KM, Tyler WS, Hennesy SM, Dominguez JJ, Last JA. 1987. Long-term consequences of exposure to ozone: II. Structural alterations in lung collagen of monkeys. Toxicol Appl Pharmacol 89:314–322.

Schraufnagel DE, Claypool WC, Fahey PJ, Jacobs ER, Rubin DB, Snider GL. 1987. Summary: Markfield

symposium. Interstitial pulmonary fibrosis. Am Rev Respir Dis 136:1281–1284.

Tyler WS, Tyler NK, Last JA, Gillespie MJ, Barstow TJ. 1988. Comparison of daily and seasonal exposures of young monkeys to ozone. Toxicology 50:131–144.

U.S. Environmental Protection Agency. 1986. Air quality criteria for ozone and other photochemical oxidants (5 volumes). EPA-600/8-84/020dF. Environmental Criteria and Assessment Office, Research Triangle Park, NC.

Weibel ER. 1979. Stereological Methods, Vol. I. Academic Press, Orlando, FL.

This morphometric study compared alterations in the amounts of components of the alveolar interstitium after 18-month exposures to either ozone or nitrogen dioxide. Special staining techniques were applied to tissue sections to enhance the appearance and subsequent identification of collagens and elastin in the interstitium. Using electron microscopy, the investigators quantified amounts of collagen fibers, elastin, basement membranes, and the remaining noncellular space in the alveolar region immediately adjacent to terminal bronchioles.

Ozone exposure produced significant increases in the amounts of interstitial collagen, basement membranes, and noncellular space in this selected alveolar region, but only madest increases in elastin. Nitrogen dioxide exposure produced a similar pattern of increases, except for elastin, which decreased relative to control values. A four-month recovery period in clean air revealed interesting differences between the two oxidant exposures; alterations produced by ozone persisted, whereas nitrogen dioxide–induced changes largely were resolved.

This study demonstrates the effectiveness of combining electron microscopic morphometric methods with appropriate tissue stains to quantify subtle, but potentially important, alterations in the interstitium of alveolar walls caused by oxidant gases. These changes clearly relate to the potential for chronic exposure to these oxidant gases to cause fibrotic changes in the lungs. However, the reported differences in effects produced by ozone and nitragen dioxide suggest that injury patterns differ among oxidants. ⊞

The Health Effects Institute (HEI) is an independently governed nonprofit corporation founded in 1980 to provide objective, credible, high-quality information on the potential human health effects of motor vehicle emissions. HEI is funded equally by the U.S. Environmental Protection Agency (EPA) and 28 automotive manufacturers and marketers in the United States.



Telephone 617-621-0266 FAX 617-621-0267

**Health Effects Institute**
141 Portland Street
Cambridge, MA 02139

Nonprofit Org.
U.S. Postage
Paid
Montpelier, VT
Permit No. 62